

Hall photovoltage deep-level spectroscopy of GaN films

I. Shalish*

Division of Engineering and Applied Sciences, Harvard University, 9 Oxford St., Cambridge, Massachusetts 02138

C. E. M. de Oliveira and Yoram Shapira

Department of Electrical Engineering-Physical Electronics, Tel-Aviv University, Tel-Aviv 69978, Israel

J. Salzman

Department of Electrical Engineering, Solid State Institute and Microelectronics Research Center, Technion-Israel Institute of Technology, Haifa 32000, Israel

(Received 24 May 2001; revised manuscript received 15 August 2001; published 2 November 2001)

Spectroscopy of photoinduced changes in semiconductor Hall voltage is proposed as a method to characterize deep levels. An analytical expression for the Hall coefficient as a function of the charge trapped at grain boundaries is derived. The experimental Hall voltage is demonstrated by measuring thin films of GaN grown on sapphire and is shown to be consistent with the model. The Hall voltage spectrum is correlated to spectra from three other deep-level spectroscopies: photoluminescence, photoconductivity, and surface photovoltage, obtained under the same conditions from the same sample. Comparing spectra from the various spectroscopies shows that the yellow-luminescence-related deep states in GaN are charged in equilibrium and discharged by the exciting photons, and suggests that the blue-luminescence-related states are deep donors positioned 2.8 eV above the valence band and neutral in equilibrium.

DOI: 10.1103/PhysRevB.64.205313

PACS number(s): 73.20.Hb, 41.20.-q, 72.40.+w

I. INTRODUCTION

In recent years, technological breakthroughs in GaN growth and device technologies have resulted in numerous devices, notably the blue emitting GaN based laser¹ and the solar blind focal plane array camera.² For lack of adequate GaN substrates, GaN films are commonly grown on substrates to which they are both lattice and thermally mismatched. Typical growth process starts with the formation of a highly defective nucleation layer at temperatures lower than the typical growth temperature providing a bridge over the lattice mismatch. The following growth proceeds as islands, which evolve into columns that eventually coalesce. The resulting columnar structure is commonly observed in cross-sectional micrographs.³ A consequence of this granular structure is the high density of defects ($10^9 - 10^{10} \text{ cm}^{-3}$) typically observed in these films.⁴ A comparable defect density would inhibit lasing in GaAs. Lasing in GaN may be accounted for by the localized nature of the defects, which were shown to be located mainly at grain boundaries.⁵ To reduce the density of defects, lateral epitaxial overgrowth (LEO) has lately been incorporated.^{4,6,7} LEO enables further growth of selected grains resulting in lower density of grain boundaries. However, despite the progress, extended defects are still present in most of today's GaN devices.

Electronic states in the forbidden gap (gap states or deep levels) are the electronic expression of defects. Hence, deep level spectroscopies provide an indirect method to monitor the presence of defects through their electrical activity. Of the various spectroscopic methods used by GaN growers, photoluminescence (PL) has probably been the most common. A frequent finding is that when GaN films are exposed to above-bandgap illumination, a characteristic yellow luminescence (YL) is emitted. This luminescence appears as a

broad spectral peak, centered around $\sim 560 \text{ nm}$ (photon energy of $\sim 2.2 \text{ eV}$).⁸ Cathodoluminescence studies have shown that this YL originates at grain boundaries.⁵ A connection was also shown between the presence of YL and persistent photoconductivity.⁹ Lately, we proposed a model and provided evidence for grain-boundary controlled transport in GaN films. According to this model, YL related acceptor states, present at the GaN grain boundaries, capture electrons and are responsible for the formation of potential barriers between the grains. These states can be discharged using sufficiently energetic photons, resulting in lowering of the barriers and an increase of the lateral transport through the layer.¹⁰ Photoinduced conductivity may imply a photoinduced mobility, as these two properties are directly proportional. A common way of measuring mobility is the Hall effect. The mobility thus measured, termed the Hall mobility, is defined as the product of the Hall coefficient, R_H , and the conductivity, σ ,¹¹

$$\mu = |R_H| \sigma. \quad (1)$$

By this definition, it is clear that Hall mobility is also directly proportional to the magnitude of the Hall coefficient, R_H . In equilibrium and under constant current and magnetic field, R_H should be constant. However, as we discuss herein, it may change under photoexcitation. Studies of photoinduced mobility as a function of photon energy have been carried out on semi-insulating GaAs.¹²⁻¹⁴ Significant mobility variations were only observed under above-bandgap illumination. Several works have been reported lately which relate the observation of thermally activated mobility in both doped and undoped GaN to the presence of grain-boundary potential barriers.¹⁵⁻¹⁷

In this paper, we propose the use of photoinduced changes in the Hall coefficient as a spectroscopic tool for monitoring deep levels at internal interfaces, such as grain boundaries. To demonstrate this tool, we examine photoinduced changes of the Hall coefficient in GaN. The obtained Hall voltage spectrum is correlated to other deep-level spectroscopies (photoluminescence, surface photovoltage, and photoconductivity) obtained from the same sample. The correlation is used to characterize the underlying deep levels in GaN and to support the hypothesis of grain-boundary controlled transport mechanism in GaN films.

II. MODEL

The Hall coefficient, R_H , is inversely proportional to the carrier concentration, n :

$$R_H = -r \frac{1}{qn}, \quad (2)$$

where q is the electron charge, and r is a proportionality coefficient known as the scattering coefficient. At the low magnetic fields commonly employed in Hall measurements, $r \geq 1$ and is given by

$$r = \langle \tau^2 \rangle / \langle \tau \rangle^2, \quad (3)$$

where τ is the coherence time between subsequent impurity scattering events. Hence, the Hall coefficient relates to the *density of ionized scattering centers*, through the scattering coefficient r . Under constant magnetic field, current, and carrier concentration, changes in r should be observed through the Hall voltage, V_H , as

$$E_H = \frac{V_H}{W} = R_H JB, \quad (4)$$

where E_H is the Hall field, W is the distance between the Hall voltage measurement contacts, J is the density of the applied current, and B is the magnetic field. Therefore, as long as the carrier concentration remains unchanged, photoinduced changes of the Hall voltage (Hall photovoltage) may provide information on the equilibrium ionization state of photosensitive deep levels. In lowly doped semiconductors, the density of deep levels may be comparable to the carrier concentration and thus the photoeffect of deep levels may *not* be limited to the scattering coefficient r , but may involve a compensating influence through the carrier concentration n [Eq. (2)]. On the other hand, moderate doping is usually enough to render the photoexcited excess carriers negligible. To demonstrate the applicability of the Hall photovoltage spectroscopy, we have chosen GaN. Unintentionally doped GaN is typically moderately to heavily doped n -type ($n > 10^{16} \text{ cm}^{-3}$), while the observed densities of defects are typically a few orders of magnitude smaller ($n_t < 10^{12} \text{ cm}^{-3}$).¹⁸ This combination makes the GaN suitable for Hall photovoltage spectroscopy.

GaN presents, however, a special case, where the material is not uniform but is composed of ordered columnar grains. Hence, most of the scattering events are likely to take place at the potential barriers formed at the boundaries of the GaN

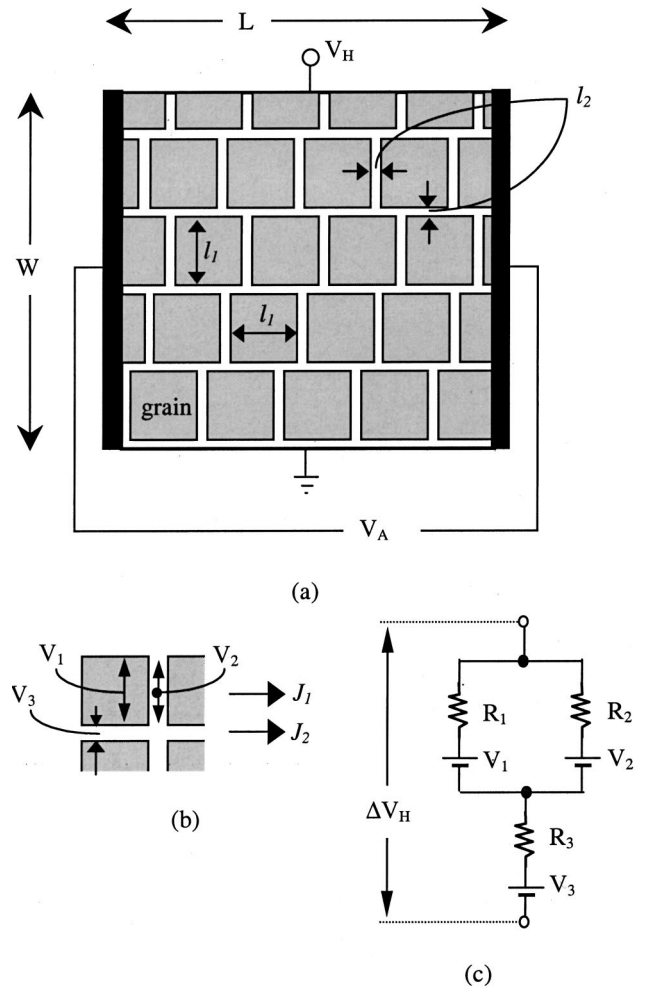


FIG. 1. (a) Schematic representation of Bube's model with grains of dimension l_1 and resistivity ρ_1 , separated by grain boundaries of dimension l_2 and resistivity ρ_2 . (b) A unit cell and the three possible voltage components of the Hall voltage produced in the cell. (c) Equivalent circuit (after R. H. Bube, Ref. 19).

grains. This special case makes it easy to obtain an expression for r using a simple model. To that end, we use a model originally introduced by Bube for the case of Hall effect in inhomogeneous materials.¹⁹ Since the GaN film is known to grow in columnar structure, it may be viewed as composed of two materials: one represents the bulk of each grain and possesses low resistivity, ρ_1 ; the other has high resistivity, ρ_2 , representing the grain boundaries, where defects trap charges and repel free carriers. The added resistivity of the grain boundaries gives rise to an additional Hall voltage produced over these boundaries. This additional Hall voltage may be expressed as a factor, $r > 1$, increasing the Hall coefficient.

Let us assume a material composed of columnar grains of square cross section with dimension l_1 and resistivity ρ_1 , separated by grain boundaries with typical thickness l_2 and resistivity ρ_2 , as illustrated in Fig. 1(a).²⁰ Assuming the GaN film can be treated as a series of basic such unit cells [Fig. 1(b)] each unit cell may be described by an equivalent circuit [Fig. 1(c)]. For this model, we also assume that no scattering

events take place inside a grain, and that if such events occurred, their overall influence on the measured Hall voltage would be negligible as compared to the scattering at the grain boundaries. Following Bube's notation, we define two dimensionless parameters, which reflect the properties of the material, $\alpha \equiv \rho_1/\rho_2$, and $\beta \equiv l_2/l_1$. In the following treatment, we assume $\beta \ll 1$.

If the Hall voltage produced at each unit cell is ΔV_H , the total Hall voltage will be given by

$$V_H = \Delta V_H W / (l_1 + l_2), \quad (5)$$

where $W/(l_1 + l_2)$ is the number of unit cells in series. In each of the unit cells, three voltages develop and contribute to the Hall voltage: V_1 is the voltage generated across the bulk of the grain, V_2 generated in parallel with V_1 across a grain boundary, and V_3 that is generated across a grain boundary in series to V_1 and V_2 . These three voltages are represented in Fig. 1(c) by three voltage sources and their series resistances. Using the equivalent circuit, we can express ΔV_H in terms of the three contributions:

$$\Delta V_H = V_1 + \frac{r_1}{r_1 + r_2} (V_2 - V_1) + V_3, \quad (6)$$

where

$$\frac{r_1}{r_1 + r_2} = \frac{\alpha\beta}{1 + \alpha\beta} = \alpha\beta, \quad (7)$$

$$V_1 = R_1 l_1 j_1 B = R_1 l_1 \frac{V_A}{L} \frac{(1 + \beta)}{\rho_1 + \beta\rho_2} B = R_1 l_1 \frac{V_A}{L} \frac{1}{\rho_1 + \beta\rho_2} B, \quad (8)$$

$$\begin{aligned} V_2 &= R_2 l_2 j_1 B = R_2 l_1 \frac{V_A}{L} \frac{(1 + \beta)}{\rho_1 + \beta\rho_2} B \beta \\ &= R_1 l_1 \frac{V_A}{L} \frac{1}{\rho_1 + \beta\rho_2} B \frac{\beta}{\alpha} = \frac{\beta}{\alpha} V_1, \end{aligned} \quad (9)$$

$$\begin{aligned} V_3 &= R_2 l_2 j_2 B = R_2 l_2 \frac{V_A}{L} \frac{1}{\rho_2} B = R_1 l_1 \frac{V_A}{L} \frac{1}{\rho_1} B \beta \\ &= \beta \frac{\rho_1 + \beta\rho_2}{\rho_1} V_1 = \beta \left(1 + \frac{\beta}{\alpha} \right) V_1, \end{aligned} \quad (10)$$

while R_1 is the Hall coefficient for the bulk of the grain, i.e., for monocrystalline GaN, and R_2 is the Hall coefficient for the grain boundaries.

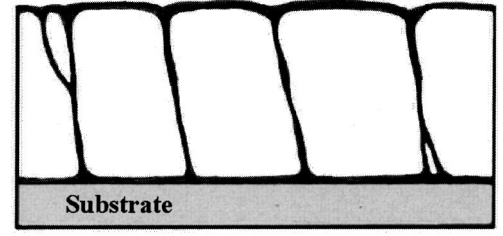
Substituting Eqs. (7) and (9) into Eq. (6) shows that for $\beta \ll 1$ we get $\Delta V_H = V_1 + V_3$. Hence, we get

$$\Delta V_H = R_1 l_1 \frac{V_A}{L} \frac{1}{\rho_1 + \beta\rho_2} B \left(1 + \frac{\beta^2}{\alpha} \right). \quad (11)$$

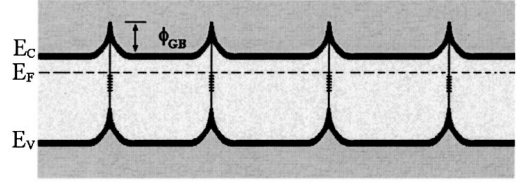
Substituting Eq. (5) into Eq. (4), we obtain a relation between the measured Hall coefficient R and ΔV_H :

$$\frac{W}{l_1 + l_2} \Delta V_H = R W J B, \quad (12)$$

where J is the total current density,



(a)



(b)

FIG. 2. (a) Schematic illustration of a film possessing a columnar grain structure, and (b) the corresponding equilibrium band diagram (ϕ : the average grain-boundary potential barrier).

$$J = \frac{j_1 + \beta j_2}{1 + \beta} = \frac{V_A}{L} \frac{(1 + \beta)\rho_2 + \beta\rho_1 + \beta^2}{(1 + \beta)(\rho_1 + \beta\rho_2)\rho_2} = \frac{V_A}{L} \left(\frac{1}{\rho_1 + \beta\rho_2} \right). \quad (13)$$

Substituting Eqs. (11) and (13) into Eq. (12) enables us to extract R ,

$$R = \left(\frac{l_1}{l_1 + l_2} \right) \left(1 + \frac{\beta^2}{\alpha} \right) R_1 = \left(1 + \frac{\beta^2}{\alpha} \right) R_1. \quad (14)$$

However, R_1 is the Hall coefficient for a bulk monocrystalline GaN without grain boundaries. Therefore, it relates to the measured Hall coefficient R through the scattering coefficient: $R = r R_1$. This allows us to obtain an expression for the scattering coefficient in the case of scattering at grain boundaries:

$$r = 1 + \frac{\beta^2}{\alpha} = 1 + \beta^2 \frac{\rho_2}{\rho_1}. \quad (15)$$

To complete this treatment, let us calculate ρ_2 , assuming it results from thermionic emission over a symmetric grain-boundary potential barrier (Fig. 2). The argumentation for thermionic emission transport over a forward biased grain-boundary barrier is the same as for a forward-biased Schottky barrier:²¹

$$j_F = C \cdot T^2 \cdot \exp\left(\frac{q(-\phi + V)}{kT}\right), \quad (16)$$

where ϕ , the barrier height, is assumed to be larger than the thermal energy kT , and V is the applied bias. However, unlike a Schottky barrier, the transport in this case is symmetrical. Based on this symmetry, the reverse current through this barrier should therefore be

$$j_R = -C \cdot T^2 \cdot \exp\left(\frac{q(-\phi - V)}{kT}\right) \quad (17)$$

and the total current crossing the barrier is

$$j = C \cdot T^2 \cdot \exp\left(-\frac{q\phi}{kT}\right) \left[\exp\left(\frac{qV}{kT}\right) - \exp\left(-\frac{qV}{kT}\right) \right] \\ = 2C \cdot T^2 \cdot \exp\left(-\frac{q\phi}{kT}\right) \sinh\left(\frac{qV}{kT}\right). \quad (18)$$

In our experiment, the voltage drop between two contacts that were ~ 8 mm apart could not exceed a few V. The average grain size is typically about $0.2 \mu\text{m}$,²² and therefore the voltage drop over each barrier was in our case very small as compared to the thermal energy kT . This reduces Eq. (18) to

$$j = 2C \cdot T^2 \cdot \exp\left(-\frac{q\phi}{kT}\right) \frac{qV}{kT}. \quad (19)$$

Hence,

$$\rho_2 \propto T^{-1} \exp\left\{\frac{q\phi}{kT}\right\} \quad \text{or} \quad \rho_2 = \rho_0 \exp\left\{\frac{q\phi}{kT}\right\}. \quad (20)$$

Substituting this result into the expression we obtained for r [Eq. (15)], we get

$$r = 1 + \beta^2 \frac{\rho_0}{\rho_1} \exp\left\{\frac{q\phi}{kT}\right\}. \quad (21)$$

This shows a dependence of r on the grain-boundary barrier potential, ϕ . However, this is not the *only* dependence, as the factor β depends on ϕ as well via l_1 . Most of l_1 is the depletion region induced by the grain-boundary charge. Solving the one-dimensional Poisson equation under the depletion approximation, it can be shown that the total width of the depletion regions in both sides of the boundary is^{10,23}

$$w = \left(\frac{2\varepsilon}{qN_d} \phi\right)^{1/2} \quad (22)$$

and since this depletion region w occupies most of l_1 ,

$$l_1^2 \approx \frac{2\varepsilon}{qN_d} \phi. \quad (23)$$

Substituting Eq. (23) into Eq. (21) we obtain

$$r = 1 + \frac{2\varepsilon}{qN_d l_2^2} \frac{\rho_0}{\rho_1} \phi \exp\left\{\frac{q\phi}{kT}\right\}. \quad (24)$$

Therefore, r increases with the average height of the grain-boundary potential barriers ϕ . This potential relates to the charge Q_T trapped at the grain boundary deep levels as $Q_T = qN_d w$, which, using with Eq. (22), gives

$$\phi = \frac{Q_T^2}{2\varepsilon qN_d}. \quad (25)$$

Hence, optically induced discharge of the grain-boundary defects may result in lowering of the grain-boundary potential barriers, and, consequently, decrease the measured Hall voltage by decreasing r . The YL-related states in GaN were suggested to be acceptors ionized in equilibrium, which

could be optically discharged and thus neutralized.^{10,24,25} Optical neutralization of the YL-related states may thus be expected to reduce the scattering and consequently the Hall voltage. The following experiment was set to examine this hypothesis.

III. EXPERIMENTAL DETAILS

The GaN films used in this work were grown using metal-organic vapor phase epitaxy on (0001) oriented 12×12 mm sapphire substrates.²⁶ The samples were $\sim 2 \mu\text{m}$ thick with an effective doping level of $n \sim 4 \times 10^{17} \text{cm}^{-3}$. Photoluminescence was excited using a HeCd laser (325 nm, 10 mW). The emitted luminescence was monochromatized, filtered, and sensed using a GaAs photomultiplier tube. Samples showing significant yellow luminescence were used for this study. Surface photovoltage (SPV) spectroscopy measurements were conducted inside a dark Faraday cage in nitrogen atmosphere. The surface photovoltage was measured by monitoring changes in the surface work function. These changes were monitored using the Kelvin probe technique. The latter measures the contact potential difference (CPD), i.e., the difference in work function, between the semiconductor free surface and a vibrating reference probe.^{27,28} The photovoltage is defined as the difference between the CPD values in the dark and under illumination. A commercial Kelvin probe (Besocke Delta Phi, Germany), with a sensitivity of ~ 1 mV, was used in all measurements. To provide a common ground for the probe and the sample, four Ohmic “back contacts” of indium were soldered on the periphery of the sample surface, while the Kelvin probe was brought to a distance of about 1 mm from the sample over the free part of the surface. One of the Ohmic contacts was used in the SPV measurement, and all four were used in the Hall effect measurement. We emphasize that as the back contacts were not illuminated, the results given below were not influenced by either defects at the metal/GaN interface or the exact resistance characteristics of the contact.²⁷

Photoconductivity (PC) and Hall photovoltage measurements were carried out within the same spectroscopic setup used for the SPV measurement and under the same conditions, using a four-point van der Pauw contact arrangement. A Keithly model 225 was used as a current source, and a GMW Magnet Systems, model 3470, 1.2-T electromagnet provided (with the employed interpole gap) a magnetic field of ~ 400 G. The gap between the magnet poles was ~ 20 mm to allow enough space for both the sample holder and a chromium coated silicon sample used as a mirror. Each Hall photovoltage spectrum was obtained by subtracting from the Hall voltage spectrum a spectrum obtained under the same conditions in the absence of magnetic field.

All measurements were carried out at room temperature and inside a dark Faraday cage. Prior to illumination, each GaN sample was maintained in the dark for an extended period to eliminate persisting effects of previous light exposure (typically ~ 12 h). The free surface of the sample was then illuminated using a 250-W tungsten-halogen lamp, or a 150-W xenon lamp, filtered through a 25-cm grating monochromator. For spectroscopic analysis, wavelengths were al-

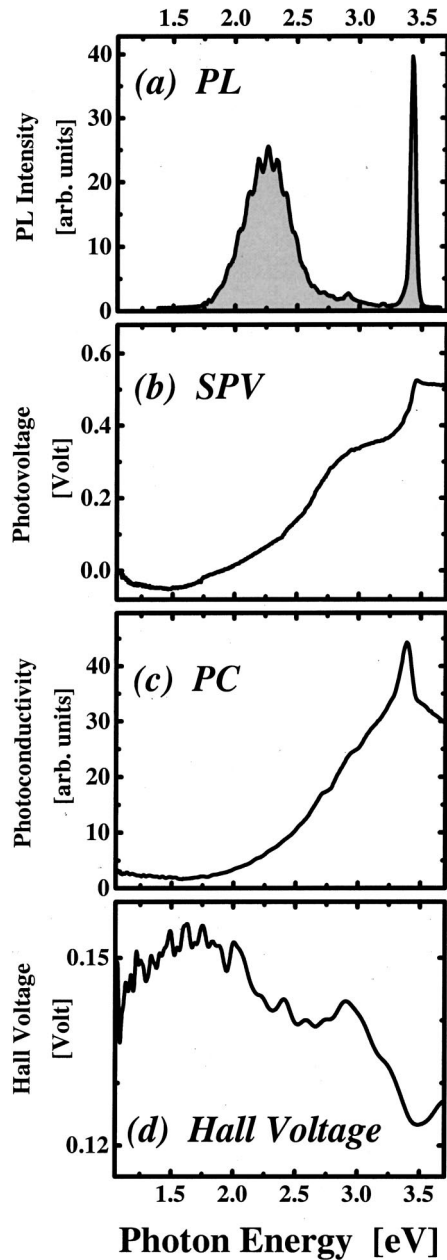


FIG. 3. (a) Photoluminescence; (b) surface photovoltage; (c) photoconductivity, and (d) Hall voltage spectra obtained from the same representative yellow-luminescent GaN sample.

ways scanned from 1200 to 350 nm, in 1-nm steps. The dwell time at each step was 60 sec and was established for these GaN films in a previous study.²⁹

The energy positions of the electron transitions observed in the various spectra were denoted by the center of the energy range, over which the transition is observed.

IV. RESULTS

Figure 3 compares spectra obtained using the four different spectroscopies on the same sample. The PL spectrum [Fig. 3(a)] features a bandgap-related peak at ~ 3.4 eV, as well as a broad below-bandgap peak, centered at ~ 2.2 eV.

This is the well-known YL peak, resulting from defect states, shown to be distributed ~ 2.2 eV below the conduction-band edge.^{10,30} A bandgap-related feature at ~ 3.4 eV is also observed at the SPV spectrum [Fig. 3(b)]. However, as SPV senses absorption, rather than emission, this feature is observed as a *knee* and not as a peak.³⁰ In the below-bandgap energy range, the SPV data feature a significant signal. It starts at ~ 1.6 eV, i.e., at the onset of the YL, and levels off at ~ 2.9 eV, i.e., at the outset of the YL. This correlation arises because SPV probes the “yellow absorption.”^{10,30} This absorption involves the transition inverse to that of the YL, i.e., the excitation of electrons from YL-related states into the conduction band.

An additional SPV transition is observed at photon energies between ~ 1 and 1.4 eV. This transition is not present in all samples. Where present, it may vary in intensity from one measurement to another and also from one sample to another. A SPV decrease in an *n*-type material typically involves a minority carrier transition,^{27,31} which in the present case implies excitation of an electron from the valence band into an empty state. This suggests that the SPV decrease is due to charging of a deep level centered ~ 1.2 eV above the valence-band edge, coinciding with that of the YL-related deep level ($E_C - 2.2$ eV = $E_V + 1.2$ eV). We therefore conclude that the two transitions at ~ 1.2 and ~ 2.2 eV are complementary transitions involving the same deep level. A sizable SPV response to a majority carrier transition, combined with a relatively weak SPV response to the complementary minority carrier transition, is commonly observed in wide band-gap semiconductors, as minority carrier transitions are known to have an inherently weaker manifestation in SPV spectra.²⁷ We note that the presence of the complementary transition indicates that the YL-related state is *not completely filled*. A transition complementary to the YL has also been observed using capacitance spectroscopy in GaN.²⁴ Finally, a transition is also observed at 2.8 eV, in correlation with a minor PL peak at the same energy. A photoluminescence peak at 2.8 eV was previously observed in GaN and is often referred to as the *blue luminescence* peak.^{32–34}

Figure 3(c) presents the photoconductivity spectrum obtained from the same sample. A bandgap-related peak at ~ 3.4 eV is observed here as well. Here, a peak is observed because at photon energies exceeding the band gap, the absorption coefficient increases considerably and most photons are absorbed in a thin near-surface layer. Thus, many generated electron-hole pairs are lost to surface recombination and the net excess carrier is decreased rather than increased.³⁵ Below the band edge a positive increase of the photoconductivity is observed starting at the same photon energy as the low-energy edge of the YL peak. A positive photoconductivity may result from the introduction of both excess electrons and excess holes. Therefore, as such, it does not reveal the energy position of the involved gap states. However, in Fig. 3(c) a small *negative* photoconductivity is observed between ~ 1.0 and 1.5 eV, i.e., exactly where the YL-complementary transition is observed in the SPV data. A negative photoconductivity is known to result only from minority carrier transitions.³⁶ If the YL-related complementary transition involves minority carriers, then the YL-related transition

at ~ 2.2 eV must involve majority carriers. Another minority carrier transition is suggested by the kink observed in the photoconductivity spectrum at 2.8 eV.

Figure 3(d) shows the Hall voltage spectrum obtained under the same excitation conditions as the SPV and the photoconductivity spectra and from the same sample. A decrease in the Hall voltage is observed to commence at the onset of the YL peak at ~ 1.5 eV, in agreement with the prediction of Sec. II. This YL-related transition clearly dominates the spectrum up to the band edge while being perturbed at 2.8 eV in correlation with the blue luminescence peak. This trend changes at the band edge, where the Hall voltage starts to increase. This increase may be explained by the limited absorption depth of above-bandgap photons: the bulk of the film is no longer excited, and a relaxation process sets in to restore the dark value of the Hall voltage. The 2.8-eV feature suggests that the deep levels related to the blue luminescence are *neutral in equilibrium*, and are charged by the light. However, the same wavelengths excite the YL-related states as well, and finally the response of the YL-related states prevails, probably due to having a stronger effect on the scattering. A transition, opposite to that of the YL, is observed over the *complementary* YL transition range ($\sim 1-1.4$ eV), in agreement with the similar transition observed both in the SPV and the PC. This type of transition is absent in samples where the complementary SPV transition and PC transition are missing.

Finally, it is important to note that GaN samples, which do not show significant below bandgap luminescence, also did not show below-bandgap transitions in spectra from the other deep-level spectroscopies used in this work.

V. DISCUSSION

Hall photovoltage spectroscopy offers information on the charging state of deep levels. While this is clearly predicted for *uniformly* distributed deep levels, the model and the results presented here show it is useful in the case of *nonuniformly* distributed deep levels, such as grain-boundary gap states. GaN provides an interesting test case.

The detailed comparison of the Hall voltage spectrum with the three spectra from the other spectroscopies strongly suggests that the decrease of the Hall voltage starting at 1.5 eV results from electronic transitions involving the YL-related states. The effects of these transitions on the conductivity, the surface photovoltage and the Hall photovoltage may all be accounted for by one model. This model relies on two well-known observations: (i) that with the current growth technology, it is only possible to produce *polycrystalline* GaN;³⁷ and (ii), that most of the YL originates at the boundaries of the GaN crystallites or grains.⁵ The presence of traps at grain boundaries led to the resurrection of the grain-boundary potential barrier model, which has been successfully used for polycrystalline silicon,³⁸ and for inhomogeneous semiconductors.³⁹ It was then shown that this model clearly accounted for persistent photoeffects in GaN, such as photoconductivity and surface photovoltage.¹⁰ The same phenomenon may, however, be explained by the metastable defect model.⁴⁰⁻⁴²

The evolution of the metastable defect model shows that several explanations other than metastable defects have been proposed. Most of these models were eventually rejected except for the “macroscopic barriers” model. In his review of *DX centers in III-V alloys*,⁴³ Lang notes that this alternative explanation “cannot be dismissed lightly,” especially in the cases of “thin ($< 5 \mu\text{m}$) epitaxial films of GaAs on semi-insulating substrates” and “impure, closely compensated bulk crystals.” The resemblance of these cases to the GaN case in hand is obvious. Nevertheless, this resemblance cannot overrule a possible presence of metastable defects in GaN. Being an ionic crystal, GaN is actually *more likely* to possess metastable defects than, e.g., GaAs.⁴³ However, unlike GaAs, GaN is polycrystalline. Hence, as long as monocrystalline GaN has not been produced, the persistent photoeffects are likely to manifest a superposition of the two mechanisms, which cannot be separated.

We show that the presence of charged grain boundaries can definitely account for a greater than unity Hall coefficient and their optical discharge for a decrease of the Hall voltage, which is also observed experimentally. These results lend further support to the applicability of the grain-boundary potential barrier model in the case of GaN thin films on sapphire.

This study offers a few “by-product” observations as well. The first one is the complementary YL transition. It is observed in SPV, PL, and Hall voltage spectra. The relative intensity of this transition was found to vary among the various methods, as well as among various samples and may even vary among various measurements of the same sample. These variations are related to the varying stages of relaxation at which a sample may be when the spectrum acquisition is begun, due to the extremely long relaxation times associated with the YL-related states in GaN.³⁰

A second by-product observation is the blue luminescence related transitions. As opposed to the YL, there is no clear evidence associating this luminescence with any specific location in the GaN film structure. The PC spectrum [Fig. 3(c)] suggests this is a minority carrier transition, while the Hall voltage spectrum suggests that the related deep level is neutral at equilibrium. As such, it is probably positioned 2.8 eV above the valence-band maximum, and is probably a nonionized donor, which may agree well with the direction of the SPV change at this energy. The evidence regarding this deep level is, yet, quite limited. Further and more specific studies are required.

Last, our model does not show any dependence of the grain-boundary barrier related part of the Hall coefficient on the magnetic field [see Eq. (24)]. Such dependence is known to exist in cases of uniformly distributed ionized impurities.⁴⁴ This dependence is commonly used to measure the Hall coefficient.⁴⁵ The absence of such dependence in the analytical expression we obtain may be of further use in identification of the relative contributions of grain-boundary charges vs uniformly distributed ionized impurities to the overall Hall coefficient. This aspect was not addressed in this work due to a lack of a sufficiently strong magnet, and therefore remains a subject for further studies.

VI. CONCLUSION

Hall photovoltage is proposed as a deep-level spectroscopy. Its power is demonstrated on GaN films.

Considerations of the common columnar grain structure of thin GaN films yield an analytical expression linking photoinduced changes of the Hall voltage with a discharge of the yellow luminescence related traps located at the grain boundaries. This linkage is shown to be generally consistent with the experimental Hall voltage spectra, in support of the grain-boundary potential barrier model in GaN.

Hall voltage spectral behavior shows that the YL related states are charged in equilibrium and may be partially discharged under illumination. Comparison of the Hall voltage

spectra with spectra from several other deep-level spectroscopies suggests that the blue luminescence related states are positioned 2.8 eV above the valence band and are deep donors neutral in equilibrium.

ACKNOWLEDGMENTS

The experimental part of this work was carried out at the Technion-Israel institute of Technology and at Tel Aviv University. This research was supported in part by the Israel Ministry of Science and by the Kidron Fund for Research in Microelectronics. Y.S. is indebted to Henry and Dina Krongold for their generous support.

*Email address: Shalish@deas.harvard.edu

- ¹S. Nakamura, Proc. SPIE **2693**, 43 (1996).
- ²J. D. Brown, Yu Zhonghai, H. Matthews, S. Harney, J. Boney, J. Schetzina, J. D. Benson, K. W. Dang, C. Terrill, T. Nohava, Yang Wei, and S. Krishnankutty, MRS Internet J. Nitride Semicond. Res. **4**, 1 (1999).
- ³P. M. Bridger, Z. Z. Bandic, E. C. Piquette, and T. C. McGill, Appl. Phys. Lett. **73**, 3438 (1998).
- ⁴B. Beaumont, P. Gibrat, M. Vaille, S. Haffouz, G. Nataf, and A. Bouille, J. Cryst. Growth **189–190**, 97 (1998).
- ⁵F. A. Ponce and D. P. Bour, Nature (London) **386**, 351 (1997).
- ⁶D. Kapolnek, S. Keller, R. Vetury, R. D. Underwood, P. Kozodoy, S. P. Den Baars, and U. K. Mishra, Appl. Phys. Lett. **71**, 1204 (1997).
- ⁷T. S. Zheleva, O. K. Nam, M. D. Bremser, and R. F. Davis, Appl. Phys. Lett. **71**, 2472 (1997).
- ⁸T. Ogino and M. Aoki, Jpn. J. Appl. Phys. **19**, 2395 (1980).
- ⁹C. V. Reddy, K. Balakrishnan, H. Okumura, and S. Yoshida, Appl. Phys. Lett. **73**, 244 (1998).
- ¹⁰I. Shalish, L. Kronik, G. Segal, Y. Shapira, S. Zamir, B. Meyler, and J. Salzman, Phys. Rev. B **61**, 15 573 (2000).
- ¹¹S. M. Sze, *Physics of Semiconductor Devices*, 2nd ed. (Wiley, New York, 1981), p. 34.
- ¹²R. H. Bube and H. E. McDonald, Phys. Rev. **128**, 2062 (1962).
- ¹³A. L. Lin, E. Omelianovski, and R. H. Bube, J. Appl. Phys. **47**, 1852 (1976).
- ¹⁴D. C. Look and E. Pimentel, Appl. Phys. Lett. **51**, 1614 (1984).
- ¹⁵J. Salzman, C. Uzan-Saguy, R. Kalish, V. Richter, and B. Meyler, Appl. Phys. Lett. **76**, 1431 (2000).
- ¹⁶Z. Bougrioua, J.-L. Farvacque, I. Moerman, P. Demeester, J. J. Harris, K. Lee, G. van Tendeloo, O. Lebedev, and E. J. Thrush, Phys. Status Solidi B **216**, 571 (1999).
- ¹⁷P. Kordos, M. Morvic, J. Betko, J. M. van Hove, A. M. Wowchak, and P. P. Chow, J. Appl. Phys. **88**, 5821 (2000).
- ¹⁸H. Morkoç, Mater. Sci. Forum **239–241**, 119 (1997).
- ¹⁹R. H. Bube, Appl. Phys. Lett. **13**, 136 (1968).
- ²⁰The cross section of the columns is typically round, while we consider square grains. We expect this difference to introduce an error, but not to affect the qualitative dependence of the Hall coefficient on the density of charges at the grain boundaries, as obtained from this simplified model.
- ²¹Reference 11, p. 256, Eq. (23).
- ²²Z. Z. Bandic, P. M. Bridger, E. C. Piquette, and T. C. McGill, Appl. Phys. Lett. **72**, 3166 (1998).
- ²³J. Y. W. Seto, J. Appl. Phys. **46**, 5247 (1975); M. Leibovitch, L. Kronik, E. Fefer, and Y. Shapira, Phys. Rev. B **50**, 1739 (1994).
- ²⁴E. Calleja, F. J. Sánchez, D. Basak, M. A. Sánchez-Garcia, E. Muñoz, I. Izpura, F. Calle, J. M. G. Tijero, J. L. Sánchez-Rojas, B. Beaumont, P. Lorenzini, and P. Gibrat, Phys. Rev. B **55**, 4689 (1997).
- ²⁵I. Shalish, L. Kronik, G. Segal, Y. Shapira, M. Eizenberg, and J. Salzman, Appl. Phys. Lett. **77**, 987 (2000).
- ²⁶J. Salzman, C. Uzan-Saguy, R. Kalish, V. Richter, and B. Meyler, Appl. Phys. Lett. **76**, 1431 (2000).
- ²⁷L. Kronik and Y. Shapira, Surf. Sci. Rep. **37**, 1 (1999).
- ²⁸A. Many, Y. Goldstein, and N. B. Grover, *Semiconductor Surfaces*, 2nd edition (North-Holland, Amsterdam, 1971).
- ²⁹The study of the dwell time effect on SPV has not been published, but some of the results were shown in Fig. 61 of Ref. 27. It is important to note that the required dwell time is derived from properties of the deep levels and therefore should be established per sample type. The response times of the samples do not vary among SPV, PC, and Hall photovoltage reported here, as all of these spectroscopies employed the same optical excitation.
- ³⁰I. Shalish, L. Kronik, G. Segal, Y. Rosenwaks, Y. Shapira, U. Tisch, and J. Salzman, Phys. Rev. B **59**, 9748 (1999).
- ³¹H. C. Gatos and J. Lagowski, J. Vac. Sci. Technol. **10**, 130 (1973).
- ³²D. M. Hofmann, D. Kovalev, G. Steude, B. K. Meyer, A. Hoffmann, L. Eckey, R. Heitz, T. Detchprom, H. Amano, and I. Akasaki, Phys. Rev. B **52**, 16 702 (1995).
- ³³M. Toth, K. Fleischer, and M. R. Phillips, Phys. Rev. B **59**, 1575 (1999).
- ³⁴M. A. Reshchikov, F. Shahedipour, R. Y. Korotkov, B. W. Wesels, and M. P. Ulmer, J. Appl. Phys. **87**, 3351 (2000).
- ³⁵H. B. DeVore, Phys. Rev. **102**, 86 (1956).
- ³⁶A. Rose, *Concepts in Photoconductivity and Allied Problems* (Wiley, New York, 1963), p. 64.
- ³⁷S. C. Jain, M. Willander, J. Narayan, and R. Van Overstraeten, J. Appl. Phys. **87**, 965 (2000).
- ³⁸J. Y. W. Seto, J. Appl. Phys. **46**, 5247 (1975).
- ³⁹H. J. Queisser and D. E. Theodorou, Phys. Rev. Lett. **43**, 401 (1979).
- ⁴⁰T. Mattila, A. P. Seitson, and R. M. Nieminen, Phys. Rev. B **54**, 1474 (1996).
- ⁴¹S. J. Xu, G. Li, S. J. Chua, X. C. Wang, and W. Wang, Appl. Phys. Lett. **72**, 2451 (1998).

- ⁴²C. Wetzel, T. Suski, J. W. Ager, III, E. R. Weber, E. E. Haller, S. Fischer, B. K. Meyer, R. J. Molnar, and P. Perlin, *Phys. Rev. Lett.* **78**, 3923 (1997).
- ⁴³D. Lang, in *Deep Centers in Semiconductors*, 2nd ed., edited by S. T. Pantelides (Gordon & Breach, Philadelphia, 1992), pp. 591–641.
- ⁴⁴D. K. Schroder, *Semiconductor Material and Device Characterization* (Wiley, New York, 1990).
- ⁴⁵G. Rutch, R. P. Devaty, W. J. Choyke, D. W. Langer, and L. B. Rowland, *J. Appl. Phys.* **84**, 2062 (1998).